Communicable Diseases Intelligence

2026 Volume 5

cdc.gov.au/cdi • Electronic publication date: 24.03.2026 • doi.org/10.33321/cdi.2026.50.015

Temporal analysis of respiratory virus epidemics in Victoria over winter 2024

Oliver Eales, Katharine L Senior, Saras M Windecker, Ruarai J Tobin, Janet Strachan, Elizabeth J Robinson, Nick Golding, James Wood, James M McCaw, Freya M Shearer

Australian Centre for Disease Control

Communicable Diseases Intelligence

Communicable Diseases Intelligence (CDI) is a peer-reviewed scientific journal published by the Australian Centre for Disease Control.

The journal aims to disseminate information on the epidemiology, surveillance, prevention and control of communicable diseases of relevance to Australia and the near region.

Submit an Article

Submit your next communicable disease related article to CDI for consideration.

Guidelines for authors and details on how to submit your publication is available on our website, or by email to the CDI Editor.

Contact us

Communicable Diseases Intelligence (CDI)

Australian Centre for Disease Control

GPO Box 798, Canberra ACT 2601

Website: **cdc.gov.au/cdi**

Email: **cdi.editor@cdc.gov.au**

ISSN: 2209-6051 Online

This journal is indexed by Index Medicus and Medline.

Original article

Abstract

During winter months of temperate regions, concurrent epidemics of multiple respiratory pathogens can occur, causing periods of increased clinical burden. Case time series, which are predominantly used to monitor infection levels, can exhibit substantial noise and day-of-the-week effects, limiting the visual interpretation of trends in raw data. However, statistical methods can infer smoothed trends within case time series by quantifying and accounting for different sources of noise. Here we apply statistical models to estimate the epidemic dynamics of SARS-CoV-2, respiratory syncytial virus (RSV), and influenza subtypes (influenza A H3N2, influenza A H1N1, and influenza B) in Victoria, Australia, over the 2024 winter season. We model trends in daily reported cases and the daily growth rate over time for all pathogens/subtypes. We present: (1) retrospective analyses using the final dataset up to 10 September 2024 and (2) weekly real-time analyses from 19 March 2024 to 10 September 2024 using data up to each timepoint, including a retrospective performance evaluation. We estimated similar peak timing of SARS-CoV-2 and RSV epidemics in late May, followed by a H3N2-dominant influenza epidemic, which peaked in early July. Transient increases in SARS-CoV-2 activity coincided with the emergence of new variants and transient decreases in influenza activity corresponded to the timing of school holidays. Real-time estimates demonstrated good agreement with those produced at the end of the season, with significant overlap of the 95% credible intervals. Our findings demonstrate how statistical methods can be implemented in real time to synthesise noisy case time-series data into interpretable trends (including uncertainty), enabling quantification of the strength of evidence for whether epidemic activity is increasing, stable or declining. Our real-time outputs were reported weekly to the Department of Health, Victoria during June–September 2024, complementing other routine surveillance indicators.

Keywords: SARS-CoV-2; RSV; influenza; influenza subtypes; respiratory pathogens

Introduction

The clinical burden from acute viral respiratory infections during winter months (in temperate climates) is most often the result of multiple concurrent epidemics.[1] The phrase “tripledemic” was coined ahead of the 2022 season in the United States of America, with some scientists and health officials highlighting the potential for influenza, respiratory syncytial virus (RSV), and SARS-CoV-2 activity to simultaneously surge, overwhelming hospital services.[2] Real-time analysis of surveillance data, including estimation of quantities such as the epidemic growth rate,[3,4] contribute to the rapid understanding of the status of concurrent epidemics and support preparation for any increased impact on healthcare services.[5]

Globally, epidemic activity of respiratory pathogens is primarily monitored using case-based surveillance systems (i.e. case reporting).[6,7] Individuals who exhibit symptoms consistent with a respiratory virus infection and presenting to healthcare providers may be tested, and a causative virus identified. In Australia, influenza, RSV, and SARS-CoV-2 are ‘notifiable’ diseases where, by law, laboratory-confirmed cases must be reported to health departments. For confirmed influenza and RSV cases, additional data may also be recorded describing the type (influenza A or B, RSV A or B) and for influenza A the subtype (influenza A H1N1 or A H3N2). Since case time series are impacted by a range of behavioural and reporting factors,[8,9] they can exhibit substantial noise and day-of-the-week effects, limiting the visual interpretation of trends in the raw data.

By accounting for different sources of noise in the observation process, statistical methods can infer smoothed trends within case time series and the uncertainty,[3,4,10,11] unlike rolling averages which do not estimate uncertainty or characterise and remove noise. From smoothed case trends, the rate of epidemic growth/decline over time and the corresponding doubling/halving times can be calculated. Both retrospective and real-time estimation of these quantities can provide useful public health intelligence. Retrospective estimates of the temporal trends in cases over a winter season support multi-season analyses, improving fundamental understanding of a pathogen's transmission dynamics, including predictions of season onset and peak timing.[12] Meanwhile, analyses conducted in real time support situational awareness, including predictions of the likely future short-term trends in epidemic activity and clinical loads.[4,13]

Here we apply statistical models to estimate the epidemic dynamics of SARS-CoV-2, RSV, and influenza subtypes in Victoria, Australia, over the 2024 winter season. We present weekly analyses from 19 March 2024 to 10 September 2024 using data up to each timepoint, and retrospective analyses using the final dataset up to 10 September 2024. Our analyses were performed in real time and were reported weekly to the Victorian Department of Health from 14 June 2024 (report 1) to 12 September 2024 (report 14).

Methods

Statistical models

We employ single-pathogen and multi-pathogen Bayesian P-spline models to infer trends within case time series, accounting for noise and day-of-the-week effects. Both models have been described in full in Eales et al 2025 (see sections 'Statistical modelling framework' and 'Supplementary Methods: Penalised-spline model').[11] We use the default Bayesian P-spline model settings used in Eales et al 2025 (i.e. basis splines of order three, five days between adjacent knots).

We use a single-pathogen Bayesian P-spline model to infer trends in the case time series of SARS-CoV-2 and RSV. The model takes as input an epidemic time series (e.g. the daily number of cases) and estimates the expected value of the time series (i.e. a smoothed trend in the daily number of cases accounting for noise) and uncertainty in the expected value (e.g. credible intervals).

For influenza, we employ a multi-pathogen Bayesian P-spline model that simultaneously considers both the total number of influenza cases and the proportions of each influenza type and subtype. The model takes as input: (1) an epidemic time series (e.g. the daily number of cases) and (2) data describing the number of tests positive for each type/subtype. The model then estimates the expected value of the epidemic time series (i.e., a smoothed trend in the daily number of cases accounting for noise) for each influenza type/subtype (A H3N2, A H1N1, B).

From the smoothed trends estimated for each pathogen we can estimate their daily epidemic growth rates over time using the equation:

$$r(t) = log(C(t)) - log(C(t-1)),$$

where $r(t)$ is the growth rate at time t (i.e. the day), and $C(t)$ is the smoothed case time series at time t. For influenza, we can also estimate the overall trend in the total epidemic time series (i.e. the sum of the modelled epidemic time-series for each influenza type/subtype).

Data

Deidentified case level data were extracted from the Victorian Department of Health notification databases: Public Health Event Surveillance System (PHESS) and Transmission and Response Epidemiology Victoria (TREVi). We use data describing the daily number of cases (by date of notification) of SARS-CoV-2, RSV, and influenza for the state of Victoria from 1 January 2023 (for SARS-CoV-2), from 18 January 2022 (for RSV), and from 1 January 2022 (for influenza) up to 10 September 2024 (for all pathogens). Influenza type (influenza A or B) was recorded for nearly all confirmed influenza cases (> 99.9%), and subtype (influenza A H3N2 or influenza A H1N1) was recorded for a small proportion (~1%) of influenza A cases (Appendix A, Figure A.1).

For RSV and influenza case data, we only use cases recorded via electronic laboratory reporting (ELR): for 2024, ELR labs represented 86.2% of positive results for influenza, and 85.3% for RSV. All modelled estimates thus reflect the expected number of (and trends in) cases recorded via ELR only. Cases not recorded using this method (~14% of case notifications in Victoria) had a delay in (manual) data entry of up to nine days during the peak period. Inclusion of those data would have biased downwards our real-time estimates of recent trends due to right truncation. All SARS-CoV-2 case data were recorded via electronic laboratory reporting.

Retrospective analysis

We present modelled estimates of the smoothed case time series, and corresponding growth rates for all pathogens, from models fitted to the entire duration of the case time series for each pathogen.

Real-time analysis

We present a series of modelled estimates from models fitted to data up to 26 selected time points from 19 March to 10 September 2024 (southern hemisphere winter), each separated by one week. Each model fit included data from the previous 365 days. The last 14 time points (12 June onwards) corresponded to the dates of our weekly reports to the Victorian Department of Health, noting that each report used data two days prior to the date of report.

During the season, data processing and statistical methods changed progressively (e.g. non-electronic records were included in the first few reports, a day-of-the-week effect was included from report two onwards). For the analyses presented here, we used consistent data (obtained on 12 September 2024), data processing and methodology to enable comparison between estimates (relative to the end-of-season estimates) across all phases of the epidemic.

This study received research ethics approval from the University of Melbourne Human Research Ethics Committee (application identifier 2024-26949-50575-3).

Results

We report on our modelled estimates of epidemic activity from daily case data (without ancillary information on the relationship between infections and cases) and therefore cannot make any inference on patterns of incident infections.

Retrospective analyses

Overall respiratory virus activity

For both SARS-CoV-2 and RSV, peak epidemic activity occurred in late May 2024 (Figure 1). Peak epidemic activity of influenza occurred later in the season, in early July. The magnitude of peak epidemic activity, in terms of modelled cases, was similar for SARS-CoV-2 and RSV (approximately 300 modelled cases per day) and relatively higher for influenza (approximately 600 modelled cases per day).

SARS-CoV-2

SARS-CoV-2 cases began increasing from mid-March 2024 (Figure 1). Following a peak in late May 2024, SARS-CoV-2 cases initially decreased sharply, though there were transient increases in the epidemic growth rate later in the season: a small uptick in the epidemic growth rate was observed in early June that stabilised just below zero (the threshold for epidemic growth/decline); another uptick occurred in mid-July which temporarily reached around zero before falling again. The peak timing and magnitude of cases in 2024 was similar to the 2023 winter season (Figure 2), noting that SARS-CoV-2 activity also surged in the summer months of 2023–2024 (Appendix A, Figure A.2).

RSV

Cases of RSV began increasing at a low rate (growth rate just above zero) in November–December 2023 (Appendix A, Figure A.3) and continued increasing at a relatively stable epidemic growth rate from January 2024 through to mid-May 2024 (Figure 1). The epidemic peaked very sharply in late May/early June, with the growth rate rapidly declining from well above to well below zero (the threshold for epidemic control) over a two-week period. Following this rapid decline in the growth rate, it remained stable and below zero until the end of the analysis period (10 September 2024). In the 2022 and 2023 winter seasons, RSV epidemics showed more gradual transition phases, with smoother epidemic peaks than in the 2024 season (Figure 2).

Figure 1: Epidemic dynamics of SARS-CoV-2, respiratory syncytial virus (RSV) and influenza over the 2024 winter season,[a] Victoria, Australia

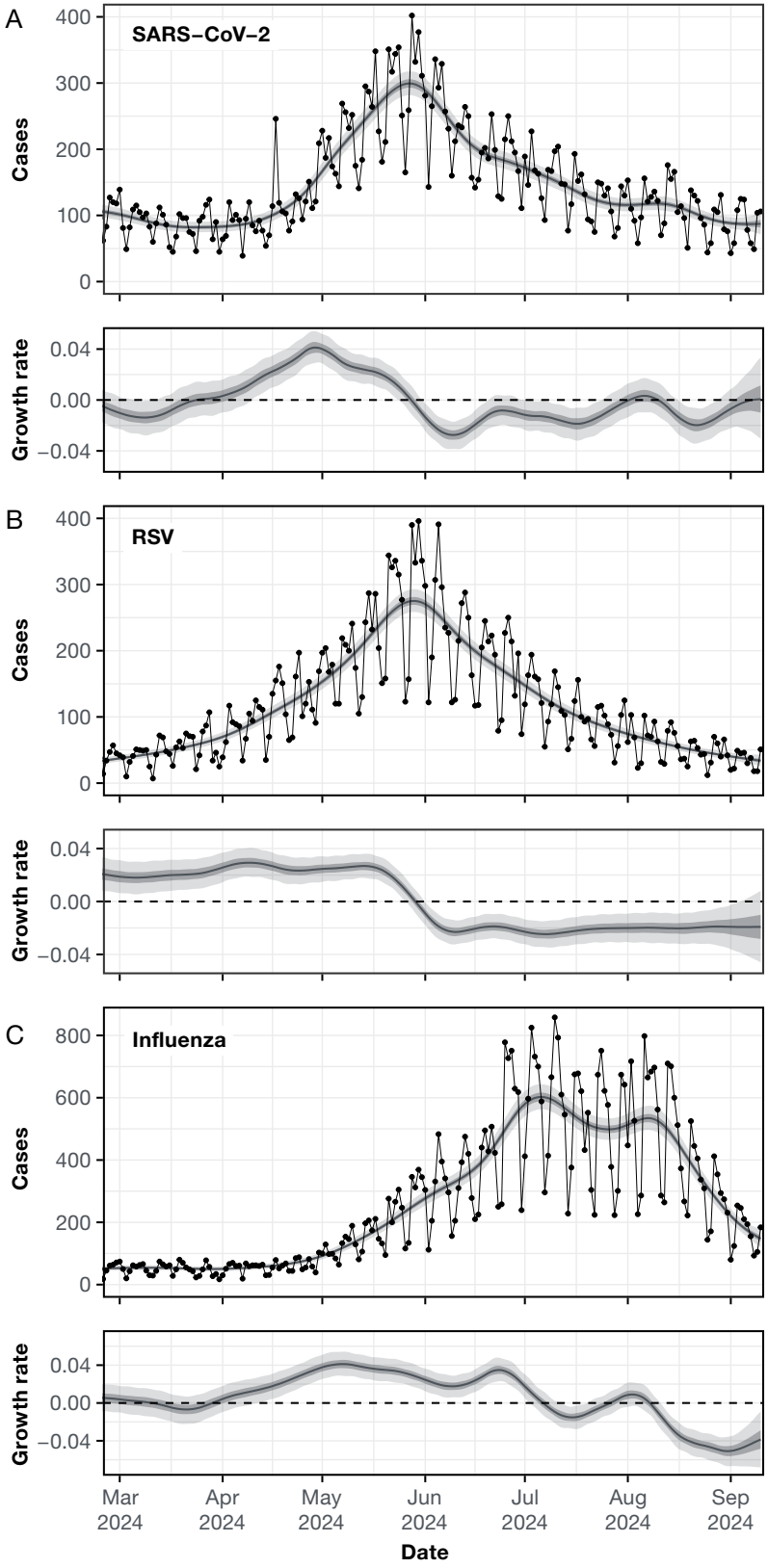

a Graphs within this figure show retrospective modelled estimates (using data up to 10 September 2024) of the expected number of cases and daily growth rate over time for: (A) SARS-CoV-2; (B) RSV; and (C) influenza. All estimates are shown over time with median (line), 50% credible intervals (dark shaded region) and 95% credible intervals (light shaded region). Also shown is the daily number of cases (black points, connected by black line); modelled estimates including day of the week effects (for better comparison to the case time series) are provided in Appendix A, Figures A.2, A.3 and A.4. The dashed line shows where growth rate equals 0, the transition point between epidemic growth and decline.

Figure 2: Comparison of the 2024 winter season with previous seasons,[a] Victoria, Australia

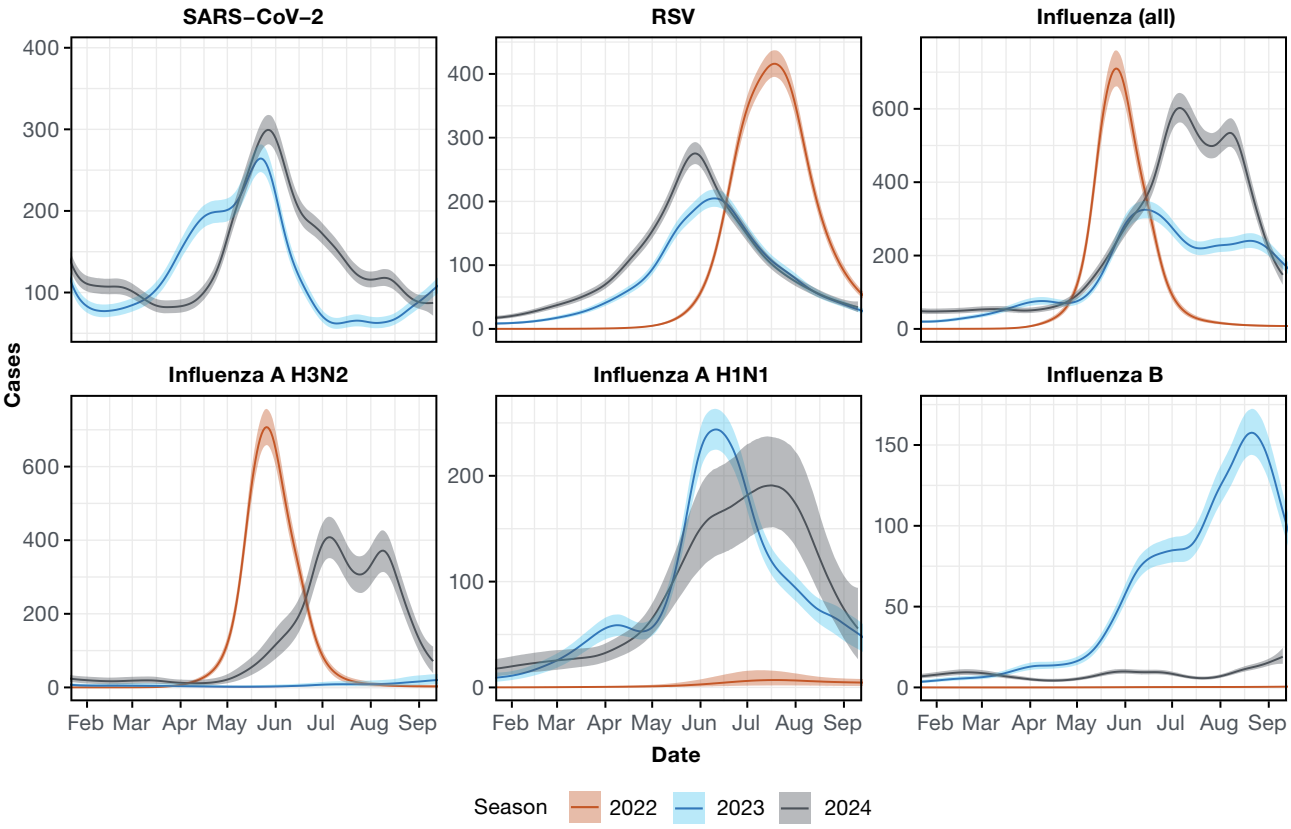

a Modelled estimates of the expected number of cases over the season for: SARS-CoV-2, respiratory syncytial virus (RSV), influenza (all), influenza A H3N2, influenza A H1N1, and influenza B. Estimates are shown for the 2024 winter season (black), the 2023 winter season (blue), and the 2022 winter season (orange). All estimates are shown over time with median (line), and 95% credible intervals (shaded region).

Influenza

Influenza cases began increasing in late March 2024 (Figure 1; Appendix A, Figure A.4). We estimate that influenza cases peaked in early July and declined for approximately 2–3 weeks. This decline was followed by a temporary uptick in the epidemic growth rate in late-July from below to just above zero; the timing of these fluctuations coincided with school holidays (29 June – 14 July 2024). This temporary increase in the epidemic growth rate led to a second peak, of similar magnitude to the first, in modelled cases in early August.

We considered the individual dynamics of three influenza types/subtypes: influenza A H3N2, influenza A H1N1, and influenza B (Figure 3). Influenza A dominated the season; based on cases with subtyping data, cases of H1N1 began increasing at a low rate (growth rate just above zero) from January 2024 (Appendix A, Figure A.5), with H1N1 dominating the early part of the influenza season relative to cases of H3N2, which only began increasing in mid-April. The epidemic growth rate of H3N2 was consistently higher than all other subtypes from early May to late-June (Figure 3). This led to H3N2 dominating the latter part of the influenza season and the period of peak influenza activity. At their peaks, H3N2 resulted in approximately 400 modelled cases per day, compared to approximately 200 cases per day for H1N1. Limited influenza B activity was observed throughout the season, with some epidemic growth occurring towards the end of the season from late July onwards; modelled influenza B cases (~20 modelled cases per day) were still lower than other influenza subtypes on 10 September.

The double peak pattern in overall modelled influenza cases was driven by patterns in modelled H3N2 cases (Figure 3). In the 2023 season there was also a double peak structure in influenza cases, but this was caused by two differently timed epidemics of influenza B and influenza H1N1 (Figure 2).

Figure 3: Epidemic dynamics of influenza subtypes over the 2024 winter season,[a] Victoria, Australia

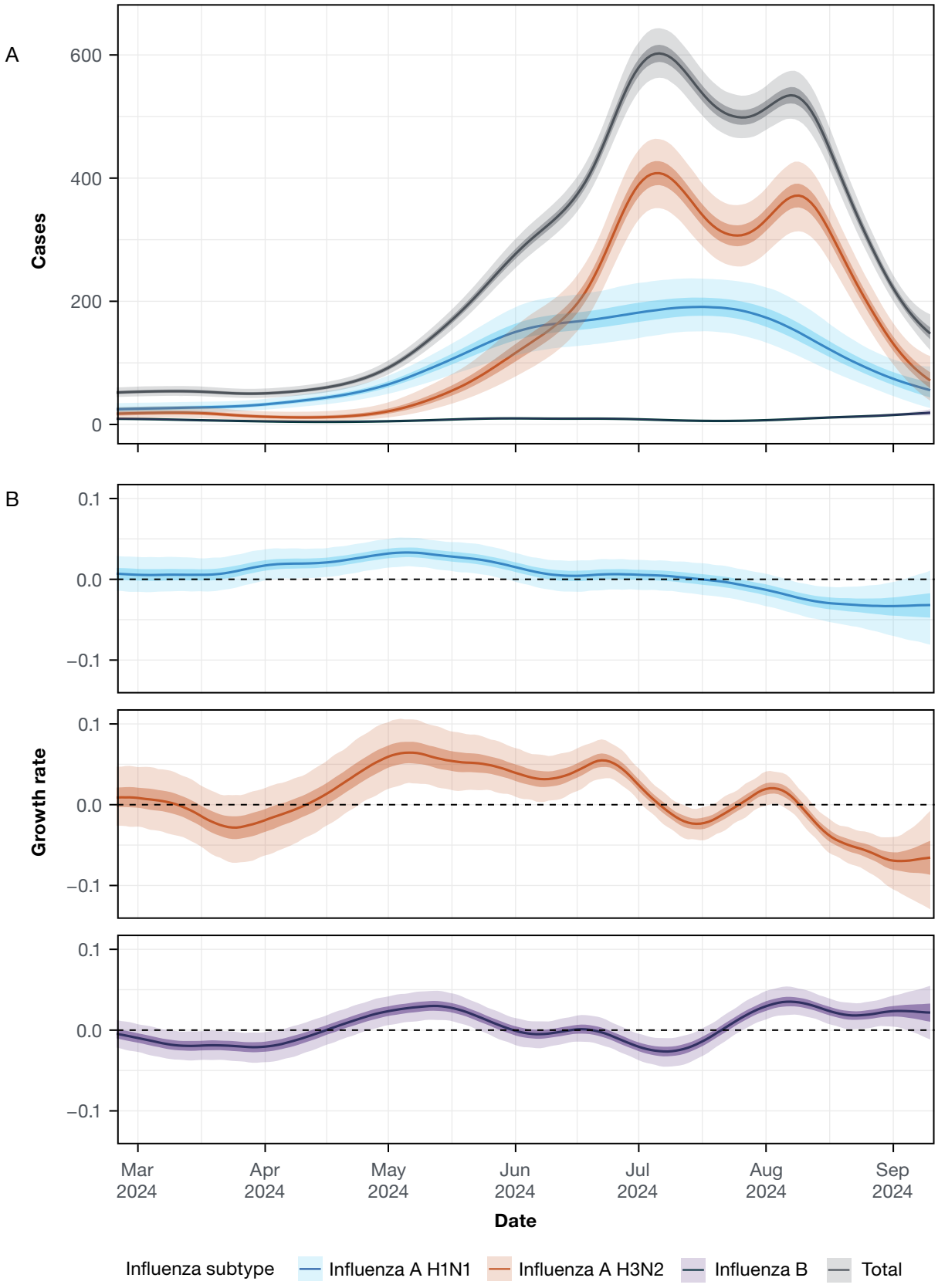

a Modelled estimates of the expected number of cases (A) and daily growth rate (B) over time for: influenza A H3N2, influenza A H1N1, and influenza B. All estimates are shown over time with median (line), 50% credible intervals (dark shaded region) and 95% credible intervals (light shaded region). The dashed line shows where growth rate equals 0, the transition point between epidemic growth and decline. Modelled estimates of the relative proportion of influenza subtypes (for better comparison to the typing/subtyping data) are provided in Appendix A, Figure A.1.

Real-time estimates

We compared end-of-season estimates with a set of 26 mid-season/real-time estimates (using only the data available up to each time point). There was significant overlap in the 95% credible intervals of our real-time estimates and end-of-season estimates of modelled cases and epidemic growth rate for SARS-CoV-2 at all time points considered (Figure 4). As expected, uncertainty in the real-time estimates increased towards the end of each time-series (due to reduced information available to the model) and 95% credible intervals were therefore generally wider for the last day of data compared to the end-of-season estimates. Real-time estimates and end-of-season estimates for RSV were broadly consistent at all time points (Figure 4) except near the epidemic peak where there was strong disagreement between the two estimates (95% credible intervals did not overlap). We attribute this to the rapid transition from epidemic growth to decline.

Real-time estimates of modelled cases and epidemic growth rate for all influenza pathogens (i.e. the total) were broadly consistent with final estimates (Figure 5). However, there were some discrepancies between the subtype-specific real-time and end-of-season estimates. During April 2024, real-time estimates suggested stable and negative growth rates for H3N2, whereas the final estimate suggested that the growth rate steadily increased and was significantly greater than zero by the end of April. This was a period when modelled cases were estimated to be very low for H3N2 and very little subtyping was occurring (~5 subtypes determined per week, Appendix A, Figure A.1). Much better agreement in subtype-specific estimates was observed from May onwards as the number of overall and subtyped cases increased as the season progressed.

Figure 4: Real-time estimates of SARS-CoV-2 and respiratory syncytial virus (RSV) dynamics over the 2024 winter season,[a] Victoria, Australia

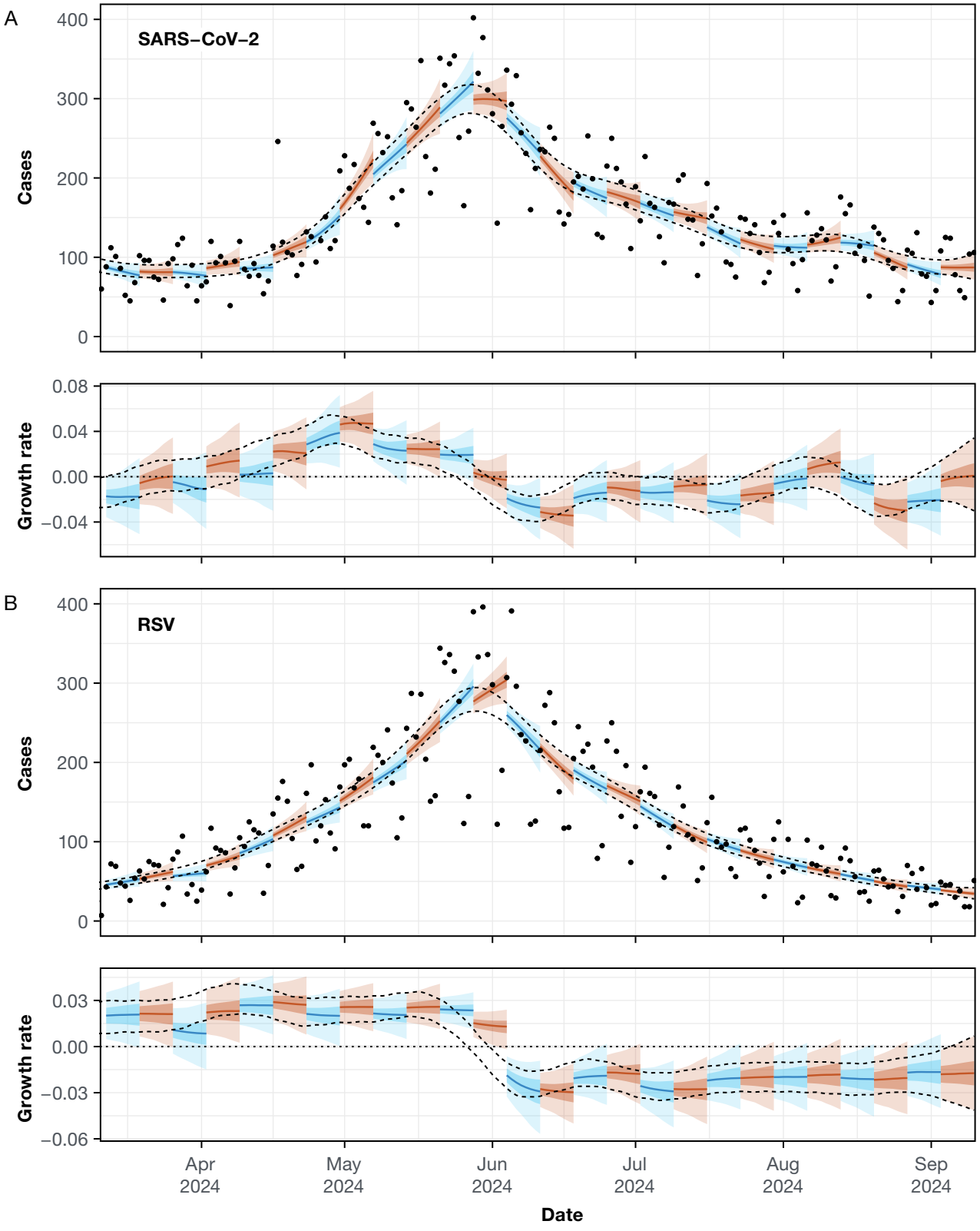

a Modelled estimates of the expected number of cases and daily growth rate over time for SARS-CoV-2 (A) and RSV (B) made at 26 different time points. All estimates (alternating colours) are shown for the last week of data. All estimates are shown over time with median (line), 50% credible intervals (dark shaded region) and 95% credible intervals (light shaded region). The two dashed lines show the 95% credible interval of modelled estimates over the entire period, estimated using data up to 10 September (the last time point). The dotted line shows where growth rate equals 0, the transition point between epidemic growth and decline.

Figure 5: Real-time estimates of influenza subtype dynamics over the 2024 winter season,[a] Victoria, Australia

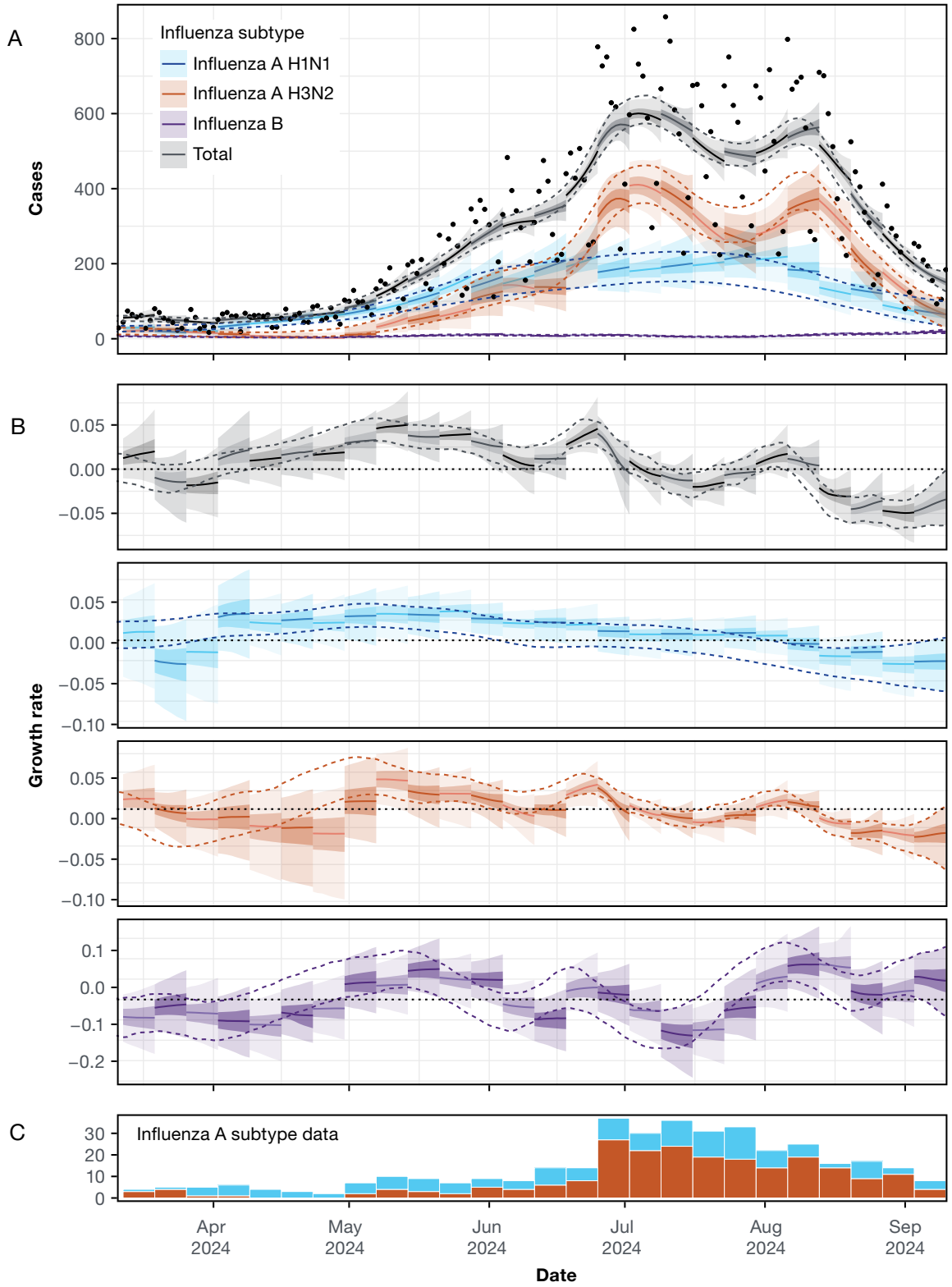

a Modelled estimates of the expected number of cases (A) and daily growth rate (B) over time for influenza A H3N2 (orange), influenza A H1N1 (blue), influenza B (green), and all influenza (i.e. the total) (black) made at 26 different time points. All estimates (alternating shades) are shown for the last week of data. All estimates are shown over time with median (line), 50% credible intervals (dark shaded region) and 95% credible intervals (light shaded region). The two dashed lines show the 95% credible interval of modelled estimates over the entire period, estimated using data up to 10 September (the last time point). The dotted line shows where growth rate equals 0, the transition point between epidemic growth and decline. (C) The raw weekly number of influenza A subtype data.

Discussion and conclusion

We have quantified the epidemic dynamics of SARS-CoV-2, RSV, and influenza in Victoria over the 2024 winter season from routinely collected case data. Our weekly real-time analyses provided smoothed estimates of trends in daily case incidence for each pathogen, accounting for noise and strong day-of-the-week effects in the raw data. From these smoothed case trends, we estimated epidemic growth rates, enabling predictions of short-term future trends in epidemic dynamics. Overall, our real-time estimates demonstrated good agreement with those produced at the end of the season (i.e. significant overlap of the 95% credible intervals), suggesting that our approach provides reliable estimates for real-time epidemic situational assessment.

Our multi-pathogen model enabled real-time monitoring of the distinct epidemic dynamics of influenza A H1N1, influenza A H3N2, and influenza B, which often exhibit different case hospitalisation ratios,[14] and which therefore have different downstream consequences on hospital loads. However, these inferred trends in influenza subtypes may be biased due to the subtyping strategies employed. While all influenza types were determined, the rate of subtyping for influenza A cases was low (~1%). It is unclear how representative these subtype samples were of the entire case dataset; subtyping may have been biased towards more severe cases and specific geographic regions. The one laboratory at which subtyping was performed services the Geelong metropolitan area and much of western Victoria. For all of 2024, this laboratory's samples represented 0.92% of the state's influenza positive samples. Additionally, any delays in subtyping would increase uncertainty in modelled estimates made using data received in real-time: the subtyping data that we received in real-time (only available for a limited number of weeks) was highly consistent with (Appendix A, Figure A.6) the final data set (used for all analyses), suggesting that subtyping delays would have made little difference to our modelled estimates. Finally, low sampling rates mean that transient features of subtype case dynamics may have been smoothed out by the statistical models employed.[11] Higher rates of sampling, and more representative sampling, could improve the validity of future analyses and could therefore improve predictive capabilities.

The epidemic dynamics of SARS-CoV-2 are likely still highly dependent on the emergence of new immune escape variants[15,16] as well as on seasonal factors.[17] SARS-CoV-2 cases began increasing in Victoria in mid-March 2024. This timing was consistent with the expansion of JN.1-descendant lineages with the F456L spike mutation in Australia, which increased in prevalence from 12.4% on the week ending 15 March 2024 to 94.6% on the week ending 11 June 2024.[18] Transient increases in the epidemic growth rate later in the season (early June and mid-July) may also have been the result of new emerging variants. For example, KP.3 descendant lineages or variants with the S31 deletion, which increased in prevalence during this period;[18] these lineages may have had a slight growth advantage over the previous lineages dominating the May/June epidemic wave. However, these transient increases may also have been caused by other effects. For example: temporary changes in contact patterns due to school holidays (see below) or weather conditions; and changes in health-care seeking behaviour or clinical PCR testing rates over time (see below). We found broadly similar timing between SARS-CoV-2 epidemics in Victoria in winter 2023 and winter 2024, which may be indicative of seasonality in SARS-CoV-2 transmission dynamics leading to more consistent timing of winter epidemics (despite there still being epidemics in summer months). However, this would require analysis of future seasons to confirm.

School holidays can influence both transmission dynamics, due to changes in social mixing patterns, and case ascertainment, due to changes in healthcare seeking behaviour. In Victoria, the inferred growth rate of influenza temporarily decreased for approximately 2–3 weeks which broadly corresponded with the school holidays (29 June – 14 July 2024), suggesting that school holidays may have influenced influenza case dynamics. This is consistent with previous studies[19–21] and with observed trends in case rates in other Australian states of New South Wales and Queensland in 2024; both states saw dramatic reductions in influenza case rates for school-aged children during their school holidays (at a similar time of the year).[22,23] Following the reopening of schools, influenza cases in Queensland rebounded in all age groups,[22] whereas in New South Wales, influenza cases

continued to decline.[23] The moderate rebound of influenza cases in Victoria perhaps suggests that when school holidays occurred the level of susceptibility in the population was higher than in New South Wales but lower than in Queensland. The transient increase in growth rate estimated for cases of SARS-CoV-2 in mid-July may also have been due to the effects of schools reopening. Although no corresponding decline in growth rate was observed when schools closed, this could be explained by simultaneous changes due to emergence of KP.3 descendant lineages (see above). RSV saw no discernible change in growth rate over this period, which may reflect that RSV case dynamics are driven by younger age groups[24] that are less affected by school holidays. In future, our analysis could be extended to consider age-specific case dynamics.

Temporal trends in case numbers reflect a combination of temporal trends in infection rates (i.e. transmission dynamics) and in case ascertainment. Since we only analysed case data, we can only infer trends in case dynamics; these trends may only partially reflect underlying trends in infections.[6] The case data used in our study consists of notified laboratory confirmed infections (by date of notification), which can be biased by: changes over time in the probability of infected individuals seeking healthcare; changes over time in the probability of laboratory testing being performed, given presentation to healthcare; and differences in transmission dynamics and behaviour between age groups.[7] Even in the absence of these biases, changes in the case time series will likely be lagged (due to delays from infection to testing and reporting)[25] and smoothed compared to actual infection incidence; this will lead to estimates of the case growth rate being lagged and smoothed compared to the infection growth rate.[26]

Real-time statistical analysis can synthesise noisy case time-series data into interpretable trends (including uncertainty). These trend analyses are often cited by public health decision-makers as evidence for decisions taken during epidemics (see, for example, reference 27). The model-based inference and growth rate estimates employed here enable quantification of the strength of evidence for whether epidemic activity is increasing, stable, or declining and can disentangle trends in multiple pathogen subtypes (where subtype-specific data are available). Such outputs can support predictions of short-term future trends in epidemic activity[28] and longer-term projections of epidemic impact, ultimately improving the ability for public health agencies to anticipate and respond to epidemic diseases.

Acknowledgments

This research is supported by the Australian Consortium of Epidemic Forecasting and Analytics (ACEFA), a National Health and Medical Research Council of Australia Centre of Research Excellence (2035303).

OE is supported by a University of Melbourne McKenzie fellowship (503965). FMS is supported by the National Health and Medical Research Council of Australia through the Investigator Grant Scheme (Emerging Leader Fellowship, 2021/GNT2010051). JMM is supported by the Australian Research Council through the Laureate Fellowship Scheme (FL240100126). FMS and JMM's research is also supported by an Australian Research Council Discovery Project Grant (DP240102286).

We wish to acknowledge the medical practitioners and pathology services who diagnosed and notified the cases to the Department of Health, Victoria. We also acknowledge the public health officers, medical officers, epidemiologists and systems specialists who have also contributed to the collection & curation of this dataset.

Data and code availability

The code for reproducing all analyses and figures is available online.[i]

All analyses were performed in the R statistical computing environment (version 4.2.3).[29] All models were fitted using the package rstan (version 2.32.6).[30] Figures were generated using the packages ggplot2 (version 3.5.1),[31] patchwork (version 1.2.0),[32] and RColorBrewer (version 1.1.3).[33]

i https://github.com/acefa-hubs/SitAssessmentPaper2024.

Author details

Dr Oliver Eales,[1,2]

Dr Katharine L Senior,[1,3]

Dr Saras M Windecker,[3]

Mr Ruarai J Tobin,[1,2]

Ms Janet Strachan,[4]

Ms Elizabeth J Robinson,[4]

Prof. Nick Golding,[1,3,5]

Prof. James Wood,[6]

Prof. James M McCaw,[1,2]

A/Prof. Freya M Shearer[1,3]

1. Infectious Disease Dynamics Unit, Centre for Epidemiology and Biostatistics, Melbourne School of Population and Global Health, The University of Melbourne, Australia
2. School of Mathematics and Statistics, The University of Melbourne, Australia
3. Infectious Disease Ecology and Modelling, The Kids Research Institute, Perth, Australia
4. Community and Public Health, Department of Health, Victoria, Australia
5. School of Population Health, Curtin University, Australia
6. School of Population Health, Faculty of Medicine and Health, UNSW Sydney, New South Wales, Australia

Corresponding author

Dr Oliver Eales

Melbourne School of Population and Global Health, 207 Bouverie St, Carlton, VIC, 3053

Phone: +61 3 9035 5511

Email: oliver.eales@unimelb.edu.au

References

1. Eales O, Plank MJ, Cowling BJ, Howden BP, Kucharski AJ, Sullivan SG et al. Key challenges for respiratory virus surveillance while transitioning out of acute phase of COVID-19 pandemic. *Emerg Infect Dis*. 2024;30(2):e230768. doi: https://doi.org/10.3201/eid3002.230768.
2. Cohen J. Will viral interference hold off the tripledemic? *Science*. 2022;378(6622):814–5. doi: https://doi.org/10.1126/science.adf8989.
3. Parag KV, Thompson RN, Donnelly CA. Are epidemic growth rates more informative than reproduction numbers? *J R Stat Soc Ser A Stat Soc*. 2022:10.1111/rssa.12867. doi: https://doi.org/10.1111/rssa.12867.
4. Eales O, Ainslie KEC, Walters CE, Wang H, Atchison C, Ashby D et al. Appropriately smoothing prevalence data to inform estimates of growth rate and reproduction number. *Epidemics*. 2022;40:100604. doi: https://doi.org/10.1016/j.epidem.2022.100604.
5. Pei S, Shaman J. Aggregating forecasts of multiple respiratory pathogens supports more accurate forecasting of influenza-like illness. *PLoS Comput Biol*. 2020;16(10):e1008301. doi: https://doi.org/10.1371/journal.pcbi.1008301.
6. Eales O, McCaw JM, Shearer FM. Challenges in the case-based surveillance of infectious diseases. *R Soc Open Sci*. 2024;11(8):240202. doi: https://doi.org/10.1098/rsos.240202.
7. Eales O, McCaw JM, Shearer FM. Biases in routine influenza surveillance indicators used to monitor infection incidence and recommendations for improvement. *Influenza Other Respi Viruses*. 2024;18(12):e70050. doi: https://doi.org/10.1111/irv.70050.
8. Moss R, Zarebski AE, Carlson SJ, McCaw JM. Accounting for healthcare-seeking behaviours and testing practices in real-time influenza forecasts. *Trop Med Infect Dis*. 2019;4(1):12. doi: https://doi.org/10.3390/tropicalmed4010012.
9. Eales O, Teo M, Price DJ, Hao T, Ryan GE, Senior KL et al. Temporal trends in test-seeking behaviour during the COVID-19 pandemic. *Math Med Life Sci*. 2025;2(1). doi: https://doi.org/10.1080/29937574.2025.2521858.
10. Abbott S, Hellewell J, Thompson RN, Sherratt K, Gibbs HP, Bosse NI et al. Estimating the time-varying reproduction number of SARS-CoV-2 using national and subnational case counts. *Wellcome Open Res*. 2020;5:112. doi: https://doi.org/10.12688/wellcomeopenres.16006.2.
11. Eales O, Windecker SM, McCaw JM, Shearer FM. Inferring temporal trends of multiple pathogens, variants, subtypes or serotypes from routine surveillance data. *Am J Epidemiol*. 2025;kwaf119. doi: https://doi.org/10.1093/aje/kwaf119.
12. Baumeister E, Duque J, Varela T, Palekar R, Couto P, Savy V et al. Timing of respiratory syncytial virus and influenza epidemic activity in five regions of Argentina, 2007–2016. *Influenza Other Respir Viruses*. 2019;13(1):10–7. doi: https://doi.org/10.1111/irv.12596.
13. Reich NG, McGowan CJ, Yamana TK, Tushar A, Ray EL, Osthus D et al. Accuracy of real-time multi-model ensemble forecasts for seasonal influenza in the U.S. *PLoS Comput Biol*. 2019;15(11):e1007486. doi: https://doi.org/10.1371/journal.pcbi.1007486.
14. Pelat C, Lasserre A, Xavier A, Turbelin C, Blanchon T, Hanslik T. Hospitalization of influenza-like illness patients recommended by general practitioners in France between 1997 and 2010. *Influenza Other Respir Viruses*. 2013;7(1):74–84. doi: https://doi.org/10.1111/j.1750-2659.2012.00356.x.
15. Jeworowski LM, Mühlemann B, Walper F, Schmidt ML, Jansen J, Krumbholz A et al. Humoral immune escape by current SARS-CoV-2 variants BA.2.86 and JN.1, December 2023. *Euro Surveill*. 2024;29(2):2300740. doi: https://doi.org/10.2807/1560-7917.ES.2024.29.2.2300740.
16. Lewnard JA, Mahale P, Malden D, Hong V, Ackerson BK, Lewin BJ et al. Immune escape and attenuated severity associated with the SARS-CoV-2 BA.2.86/JN.1 lineage. *Nat Commun*. 2024;15(1):8550. doi: https://doi.org/10.1038/s41467-024-52668-w.
17. Gavenčiak T, Monrad JT, Leech G, Sharma M, Mindermann S, Bhatt S et al. Seasonal variation in SARS-CoV-2 transmission in temperate climates: a Bayesian modelling study in 143 European regions. *PLoS Comput Biol*. 2022;18(8):e1010435. doi: https://doi.org/10.1371/journal.pcbi.1010435.

18. covSPECTRUM. Detect and analyze variants of SARS-CoV-2: Australia 2024. [Website.] Zurich: Eidgenössische Technische Hochschule Zürich, cov-spectrum.org; 2021. [Accessed on 18 November 2024.] Available from: https://cov-spectrum.org/explore/Australia/AllSamples/Y2024.

19. Ewing A, Lee EC, Viboud C, Bansal S. Contact, travel, and transmission: the impact of winter holidays on influenza dynamics in the United States. *J Infect Dis*. 2017;215(5):732–9. doi: https://doi.org/10.1093/infdis/jiw642.

20. He C, Norton D, Temte JL, Barlow S, Goss M, Temte E et al. Effect of planned school breaks on student absenteeism due to influenza-like illness in school aged children—Oregon School District, Wisconsin September 2014–June 2019. *Influenza Other Respir Viruses*. 2024;18(1):e13244. doi: https://doi.org/10.1111/irv.13244.

21. Jackson C, Vynnycky E, Mangtani P. The relationship between school holidays and transmission of influenza in England and Wales. *Am J Epidemiol*. 2016;184(9):644–51. doi: https://doi.org/10.1093/aje/kww083.

22. Queensland State Government Department of Health (Queensland Health). *Queensland acute respiratory infection surveillance report 1 January – 11 August 2024*. Brisbane: Queensland Health; August 2024. [Accessed in August 2024.] Available from: https://www.health.qld.gov.au/clinical-practice/guidelines-procedures/diseases-infection/surveillance/reports/flu.

23. New South Wales State Government Department of Health (NSW Health). *NSW Respiratory Surveillance Report – week ending 10 August 2024*. Sydney: NSW Health; 10 August 2024. Available from: https://www.health.nsw.gov.au/Infectious/covid-19/Documents/respiratory-surveillance-20240727.pdf.

24. Hogan AB, Glass K, Moore HC, Anderssen RS. Exploring the dynamics of respiratory syncytial virus (RSV) transmission in children. *Theor Popul Biol*. 2016;110:78–85. doi: https://doi.org/10.1016/j.tpb.2016.04.003.

25. Gostic KM, McGough L, Baskerville EB, Abbott S, Joshi K, Tedijanto C et al. Practical considerations for measuring the effective reproductive number, Rt. *PLoS Comput Biol*. 2020;16(12):e1008409. doi: https://doi.org/10.1371/journal.pcbi.1008409.

26. Eales O, Riley S. Differences between the true reproduction number and the apparent reproduction number of an epidemic time series. *Epidemics*. 2024 Mar 1;46:100742. doi: https://doi.org/10.1371/journal.pcbi.1008409.

27. Burton T. NSW perilous as modelling suggests Victoria slowly flattening curve. [Online news article.] Sydney: Nine Entertainment, Australian Financial Review; 17 July 2020. [Accessed on 20 January 2025.] Available from: https://www.afr.com/politics/federal/nsw-perilous-as-modelling-suggests-victoria-slowly-flattening-curve-20200717-p55cz7.

28. Moss R, Price DJ, Golding N, Dawson P, McVernon J, Hyndman RJ et al. Forecasting COVID-19 activity in Australia to support pandemic response: May to October 2020. *Sci Rep*. 2023;13(1):8763. doi: https://doi.org/10.1038/s41598-023-35668-6.

29. R Core Team. R: A Language and Environment for Statistical Computing. [Application.] Vienna: R Foundation for Statistical Computing; 2023. Available from: https://www.R-project.org/.

30. Guo J, Gabry J, Goodrich B, Johnson A, Weber S, Stan Development Team. RStan: the R interface to Stan. [Application.] 2020. Available from: https://mc-stan.org/rstan/.

31. Wickham H. ggplot2: *Elegant Graphics for Data Analysis*. 2nd ed. New York: Springer-Verlag, 2016. Available from: https://ggplot2-book.org/.

32. Pedersen TL. *patchwork: The Composer of Plots*. [Software.] 2024. Available from: https://patchwork.data-imaginist.com.

33. Neuwirth E. *RColorBrewer: ColorBrewer Palettes*. 2022. Available from: https://CRAN.R-project.org/package=RColorBrewer.

Appendix A

Figure A.1: Relative proportions of influenza subtypes from January 2022 – September 2024,[a] Victoria, Australia

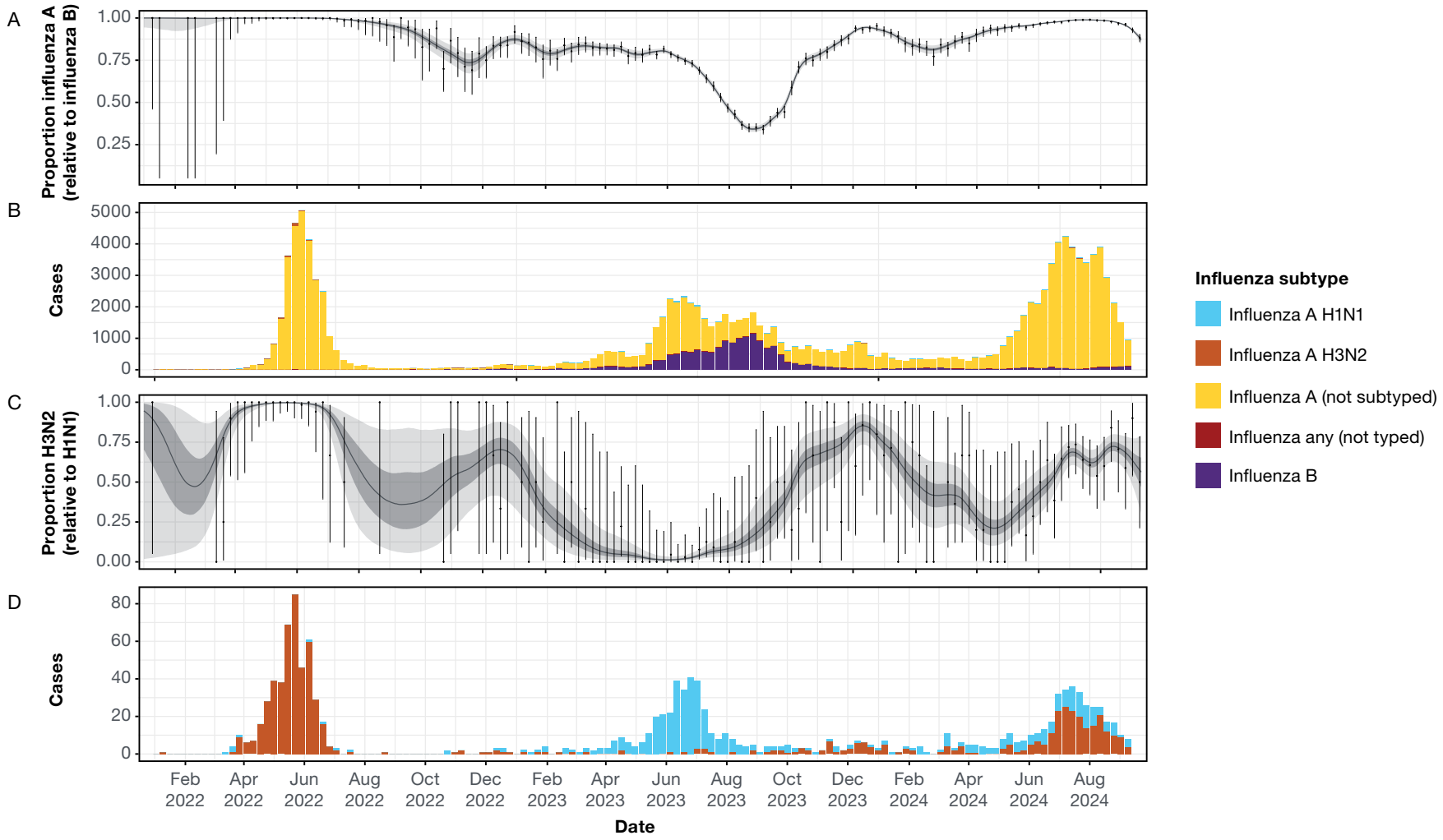

a Modelled estimates of the proportion of influenza cases caused by influenza A (relative to influenza B) (A) and the proportion of influenza A cases caused by influenza A H3N2 (relative to influenza A H1N1) (C). All estimates are shown over time with median (line), 50% credible intervals (dark shaded region) and 95% credible intervals (light shaded region). Raw weekly proportions are shown (black points) with 95% binomial confidence intervals (error bars). The raw weekly influenza typing/subtyping data is shown in (B) and (D), where (D) only includes influenza A H3N2 and influenza A H1N1 samples. Daily data was used in all models — we have shown weekly values only for easier visualisation.

Figure A.2: Epidemic dynamics of SARS-CoV-2 from January 2023 – September 2024,[a] Victoria, Australia

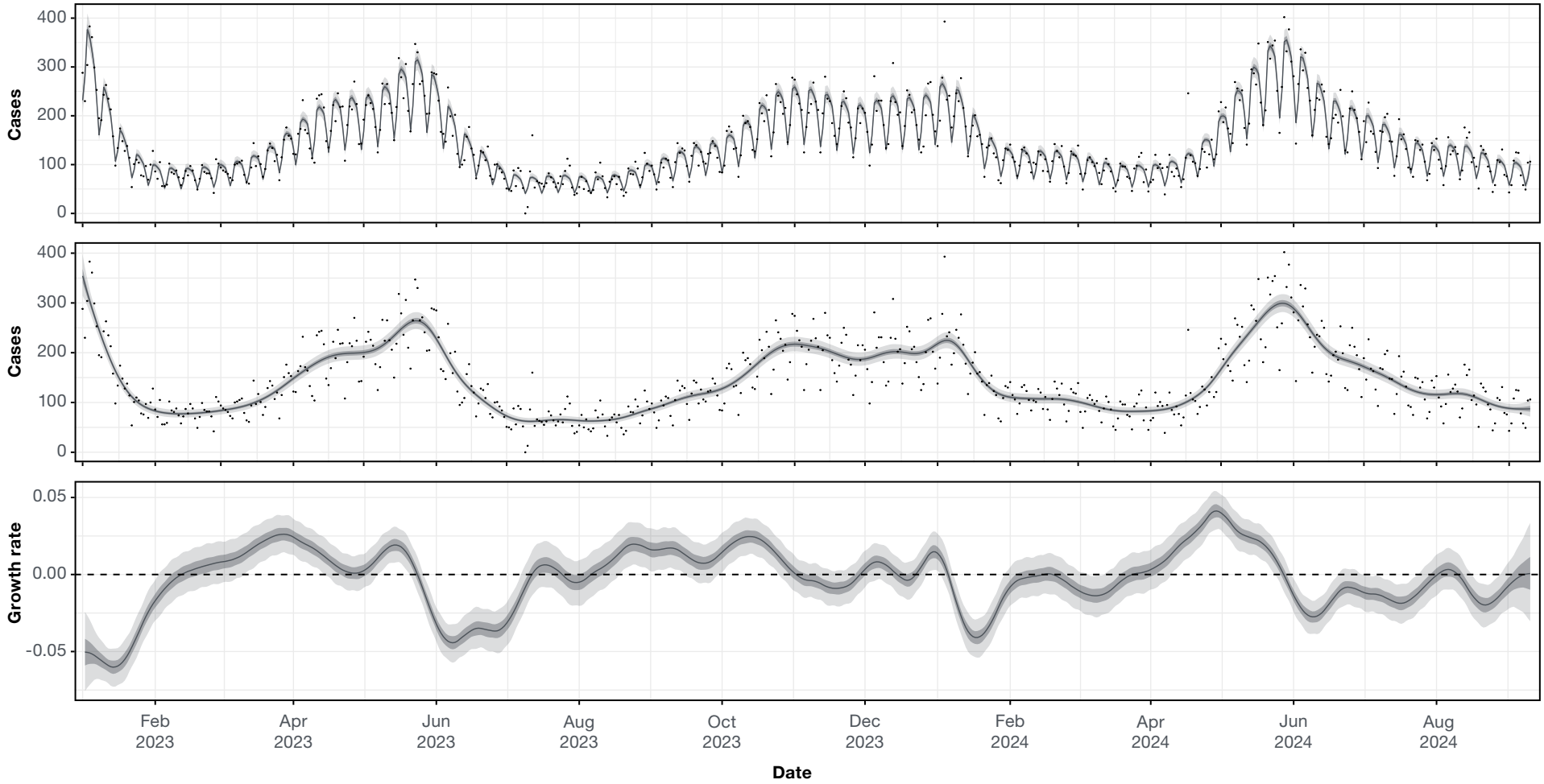

a Modelled estimates of the expected number of SARS-CoV-2 cases over time (middle panel), the expected number of SARS-CoV-2 cases over time multiplied by estimated day-of-the-week effects (top panel), and the daily growth rate of SARS-CoV-2 cases over time (bottom panel). Also shown is the daily number of cases (black points). The dashed line shows where growth rate equals 0, the transition point between epidemic growth and decline. All estimates are shown over time with median (line), 50% credible intervals (dark shaded region) and 95% credible intervals (light shaded region).

Figure A.3: Epidemic dynamics of respiratory syncytial virus (RSV) from January 2022 – September 2024,[a] Victoria, Australia

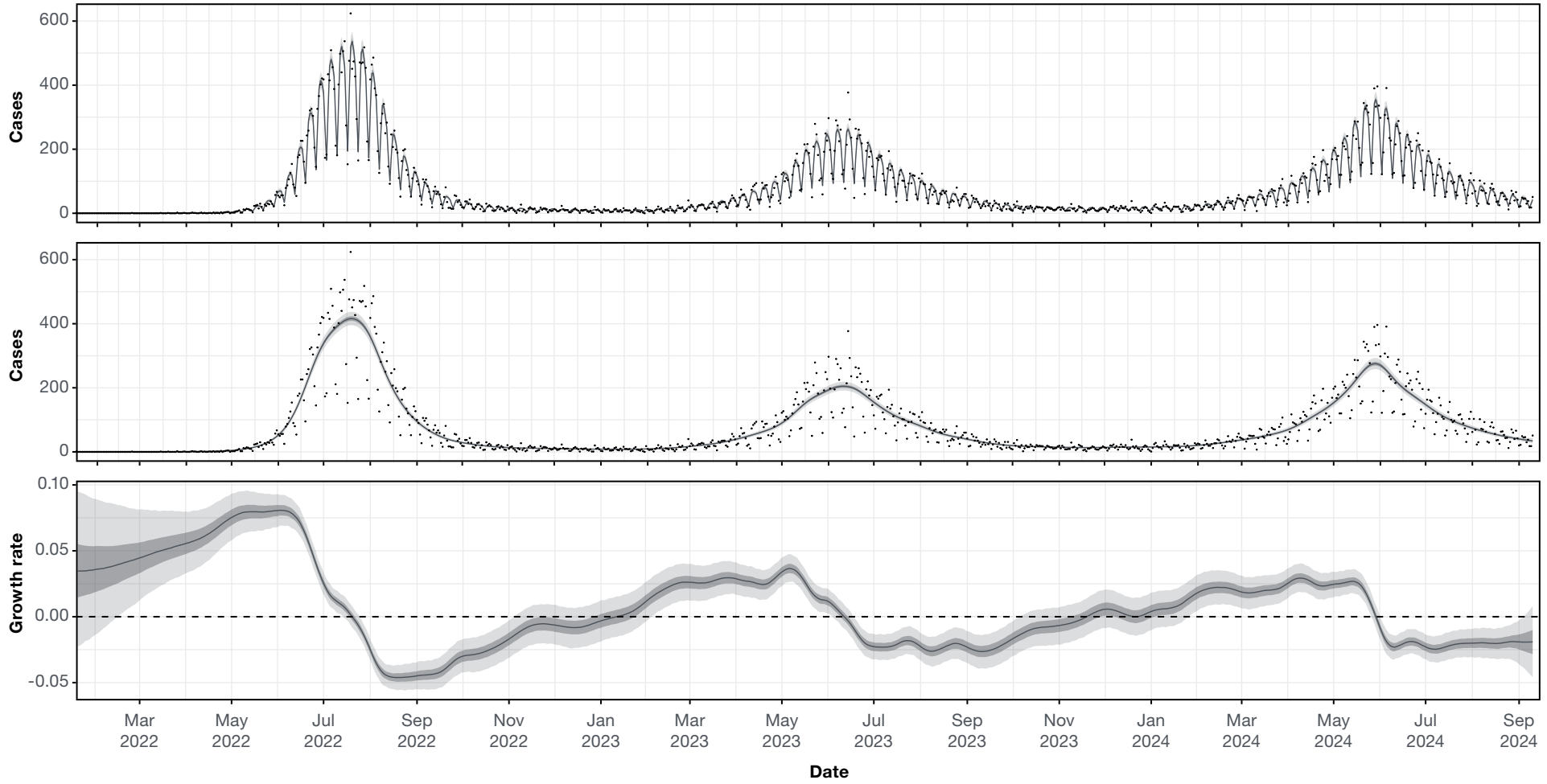

a Modelled estimates of the expected number of RSV cases over time (middle panel), the expected number of RSV cases over time multiplied by estimated day-of-the-week effects (top panel), and the daily growth rate of RSV cases over time (bottom panel). Also shown is the daily number of cases (black points). The dashed line shows where growth rate equals 0, the transition point between epidemic growth and decline. All estimates are shown over time with median (line), 50% credible intervals (dark shaded region) and 95% credible intervals (light shaded region).

Figure A.4: Epidemic dynamics of influenza from January 2022 – September 2024,[a] Victoria, Australia

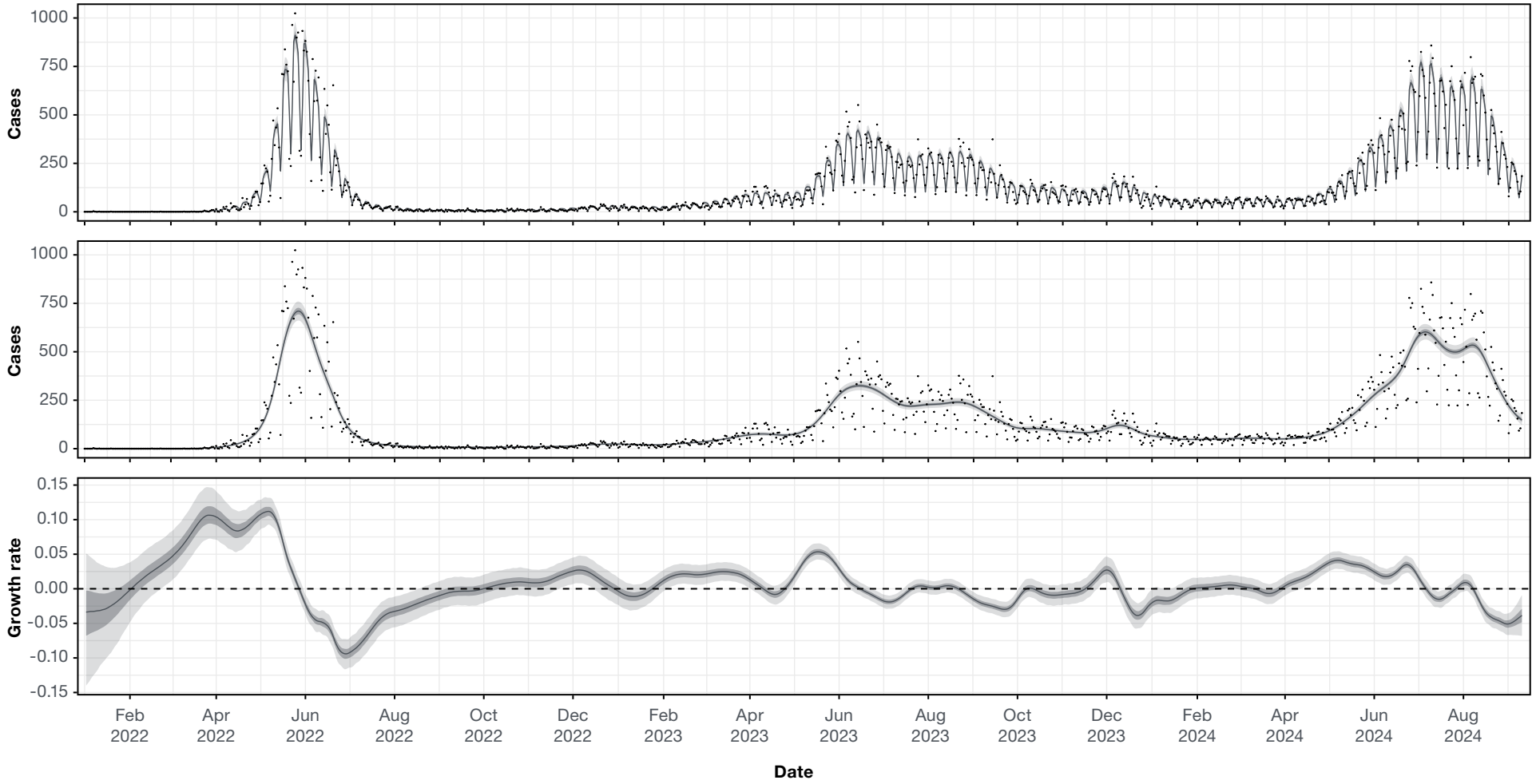

a Modelled estimates of the expected number of influenza cases over time (middle panel), the expected number of influenza cases over time multiplied by estimated day-of-the-week effects (top panel), and the daily growth rate of influenza cases over time (bottom panel). Also shown is the daily number of cases (black points). The dashed line shows where growth rate equals 0, the transition point between epidemic growth and decline. All estimates are shown over time with median (line), 50% credible intervals (dark shaded region) and 95% credible intervals (light shaded region).

Figure A.5: Epidemic dynamics of influenza subtypes from January 2022 – September 2024,[a] Victoria, Australia

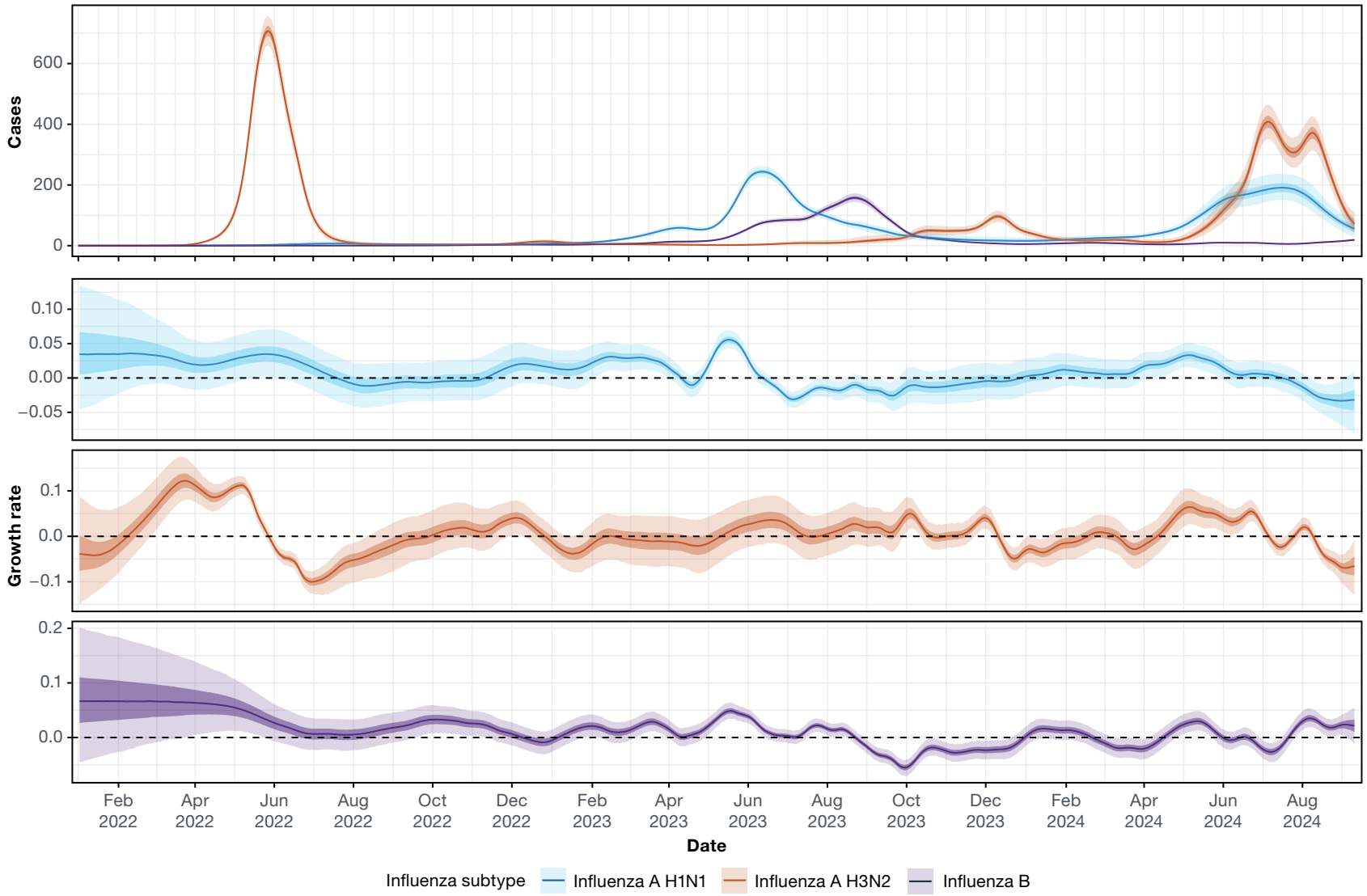

a Modelled estimates of the expected number of cases (top panel), and the daily growth rate (bottom panel) over time for influenza A H1N1 (blue), influenza A H3N2 (orange), and influenza B (purple). The dashed line shows where growth rate equals 0, the transition point between epidemic growth and decline. All estimates are shown over time with median (line), 50% credible intervals (dark shaded region) and 95% credible intervals (light shaded region).

Figure A.6: Comparison of the number of subtyped influenza A cases in data received in real-time and the final data set for the 2024 winter season,[a] Victoria, Australia

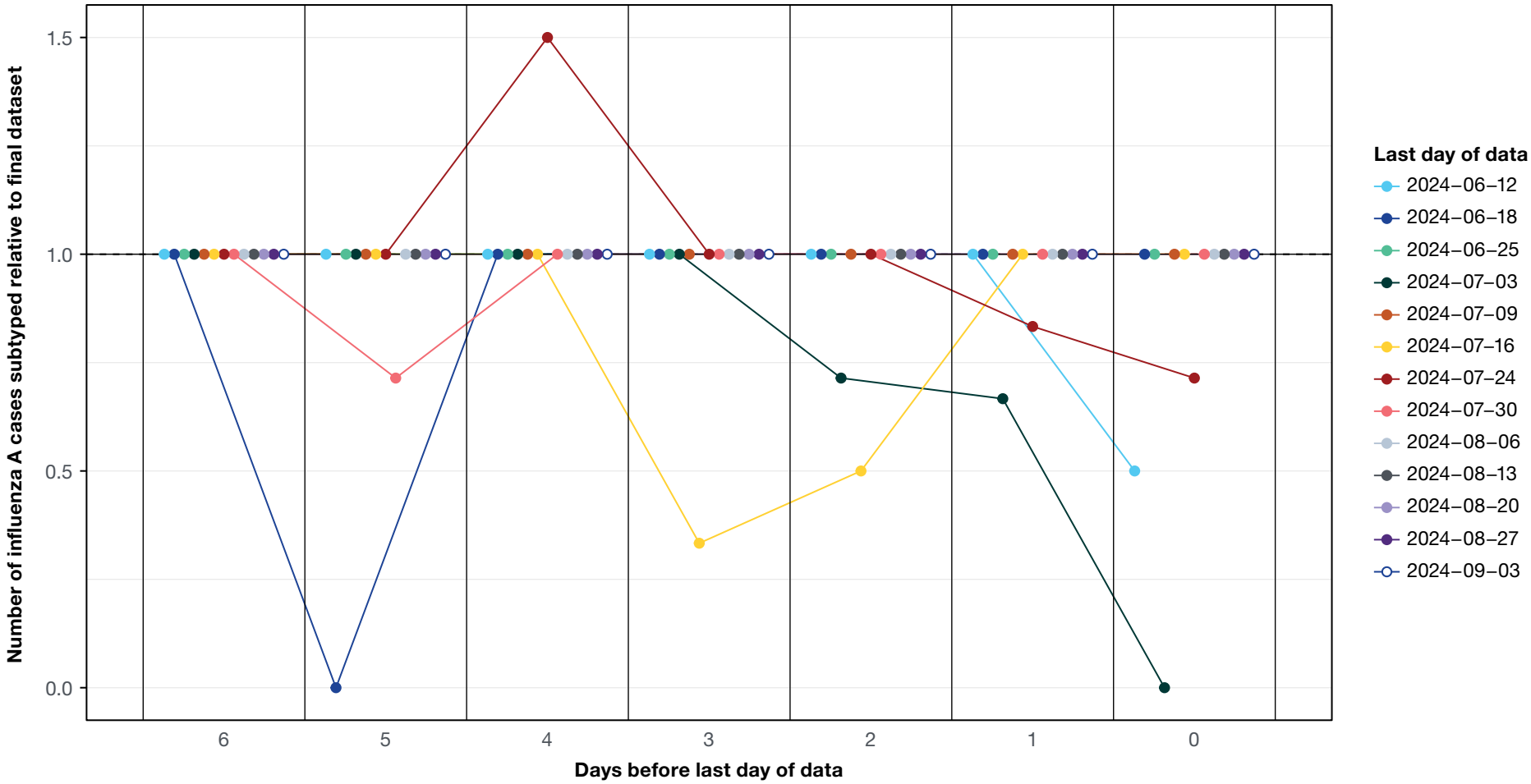

a The number of influenza A cases for which subtype (H3N2 or H1N1) data was available in data sets received in real-time during the season (by last day of data reported) relative to the final data set received 12 September 2024 (last day of data 10 September 2024). For each data set we have compared the relative number of subtypes cases for the final seven days of data. A value of 1 corresponds to no difference in the number of subtyped influenza A cases in the data received in real-time and the final dataset; note that the majority of points are at a value of 1. Values less than 1 correspond to fewer subtyped influenza A cases in the real-time data compared to the final dataset (due to occasional delays in subtyping data being received). In one instance there is a value greater than one corresponding to a greater number of subtyped influenza A cases in the real-time data compared to the final dataset; this was most likely an incorrect specification that was later corrected.